Synthesis and Characterization of Amorphous Partially Aliphatic Polyimide Copolymers Based on Bisphenol-A Dianhydride

Amy E. Eichstadt, Thomas C. Ward,* Melanie D. Bagwell, Isaac V. Farr, Debra L. Dunson, and James E. McGrath

Department of Chemistry, Virginia Tech, Blacksburg, Virginia 24061-0344

Received May 29, 2002; Revised Manuscript Received July 22, 2002

ABSTRACT: Partially aliphatic, high molecular weight polyimide copolymers were successfully synthesized using an ester−acid high-temperature solution imidization route by which noncrystalline, soluble materials were obtained. Variations in the aliphatic content produced a series of polyimides having different glass transition temperatures and processing characteristics. The ester−acid reaction pathway eliminated the need for anhydrous solvents and overcame the problem of salt formation commonly observed for nucleophilic, more basic, aliphatic amines prepared by the traditional poly(amic acid) synthesis route. Partially aliphatic polyimides containing either a cycloaliphatic diamine or aliphatic diamines with 6 or 12 methylene units were synthesized. Each copolymer was characterized by its molecular weight, glass transition temperature, thermal stability, coefficient of thermal expansion, refractive index, and dielectric constant. Structure−property relationships were established. The γ and β sub-T_g viscoelastic relaxations were explored in order to understand their molecular origins.

Introduction

Aromatic polyimides have found widespread applicability associated with their thermal stability, chemical resistance, high glass-transition temperature, and mechanical integrity.[1−3] However, wholly aromatic polyimides, though thermally stable, do not always provide the optimum properties for many specialty applications because of deficiencies in processability, solubility, and transparency as well as their relatively high dielectric constant. Previously, incorporation of aliphatic or cycloaliphatic monomers to form partially aliphatic polyimides has been used to counteract some of the shortcomings of wholly aromatic polyimides.[4−11]

Polyimides containing aliphatic groups can be organized into three categories based on the combination and types of monomers used in their synthesis: (1) aromatic dianhydrides and aliphatic diamines, (2) aliphatic dianhydrides and aromatic diamines, and (3) aliphatic dianhydrides and aliphatic diamines (i.e., fully aliphatic). In category (1), using the traditional two-step poly(amic acid) route, the basicity of the aliphatic diamine often results in the formation of insoluble intermediate salts with the carboxylic acid groups of the poly(amic acid).[4,5] As a result, it is difficult to obtain high molecular weight poly(amic acids). Salt formation can be reduced by adding the aliphatic diamine very slowly to the dianhydride[4,6,7] or by direct polycondensation in *m*-cresol at high temperatures.[8,9] Our previous work using the ester−acid high-temperature solution imidization route with aliphatic diamines produced high molecular weight, fully cyclized, soluble, amorphous, partially aliphatic polyimides without the problem of salt formation.[10] This same synthetic pathway was utilized in the present study to prepare partially aliphatic polyimides containing either (1) a cycloaliphatic diamine or (2) combinations of aliphatic diamines with 6 or 12 methylene units.

The selection of aliphatic diamine monomers for this study was based on the anticipated structure−property relations for each type of aliphatic group. Cycloaliphatic diamines impart rigidity similar to that of aromatic diamines to the polymer backbone, but offer improvements in polymer transparency and dielectric constant that are partially due to the reduced formation of charge-transfer complexes.[5,7,11,12] The linear aliphatic diamines are more flexible—the number of methylene units can determine the magnitude of the glass-transition temperature as well as the crystalline/amorphous morphology of the polyimide. When the number of methylene units within the diamine was varied from 4 to 12, other research has found an “even−odd” propensity to crystallize.[8,9] Copolymerization of rigid plus flexible monomers (aromatic, cycloaliphatic, aliphatic) has been used to control the thermal and mechanical properties of polyimides to meet specific processing and property requirements.[4,10]

The present paper discusses the synthesis and characterization of partially aliphatic copolyimides obtained from bis[4-(3,4-dicarboxyphenoxy)phenyl]propane dianhydride, or bisphenol A dianhydride (BPADA), and four diamines: 4,4’-oxydianiline (ODA), 4,4’-diaminodicyclohexylmethane (DCHM), hexamethylenediamine (HMDA), and dodecyldiamine (DoDDA). The combination of both rigid aromatic and cycloaliphatic groups with flexible aliphatic diamines in various proportions produced a systematic variation in both the thermal and mechanical properties of the polyimides. The following paper includes molecular weight, thermal, and dielectric data to establish structure−property relationships. We also discuss the molecular origins of the γ and β sub-T_g viscoelastic relaxations.

Experimental Section

Materials. *N*-Methyl-2-pyrrolidone (NMP), triethylamine (TEA), *o*-dichlorobenzene (*o*-DCB), ethanol, and methanol were used as received without further purification.

Bis[4-(3,4-dicarboxyphenoxy)phenyl]propane dianhydride, or bisphenol A dianhydride (BPADA), was donated by General Electric. 4,4’-oxydianiline (ODA) was purchased from Allco. The aliphatic diamines, isomeric 4,4’-diaminodicyclohexyl-

---

* To whom correspondence should be addressed.

10.1021/ma020835p CCC: $22.00

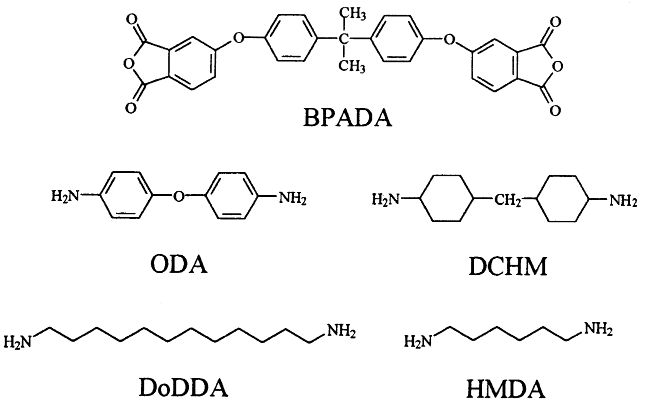

Figure 1. Monomer chemical structures.

methane (DCHM), hexamethylenediamine (HMDA), and dodecyldiamine (DoDDA) were purchased from Aldrich. All the monomer chemical structures are shown in Figure 1. Each monomer was purified by sublimation or recrystallization prior to use to ensure proper stoichiometry. After recrystallization, the BPADA was dried under vacuum at 120 °C to cyclize possible diacid moieties. ODA was dried under vacuum at 100 °C, and the HMDA and DoDDA were dried under vacuum at room temperature.

Synthesis. A number of aromatic polyimides[13−19] and partially aliphatic polyimides[10] have been prepared in our laboratories using ester−acid high-temperature solution imidization. The same approach was applied in the present study. This method involves the prereaction of aromatic dianhydrides with ethanol and a tertiary amine catalyst to form ester−acids, followed by the addition of diamines. Subsequent thermal reaction forms high molecular weight, fully cyclized polyimides. Unlike the poly(amic acid) route, the aliphatic diamines are added to the ester−acid rather than the dianhydride, thus eliminating the undesirable "gel-like" intermediate salt formation. A general reaction scheme for the BPADA/HMDA−DoDDA copolyimide is shown in Figure 2. Three BPADA-based copolyimides were synthesized by combination with the following diamine molar ratios: HMDA−ODA, 75:25; HMDA−DoDDA, 50:50; and HMDA−DoDDA, 25:75. The homopolymers BPADA/ODA and BPADA/DCHM were also prepared.

The synthesis of BPADA/HMDA−DoDDA, 50:50 is described as follows to illustrate the steps used in the ester−acid method. A three-necked round-bottomed flask was equipped with a mechanical stirrer, nitrogen inlet, and a reverse Dean−Stark trap fitted with a condenser. To the flask, 20 g (38.43 mmol) of BPADA was charged and rinsed in with 200 mL of ethanol and 6 mL of TEA. Under refluxing conditions, the ethyl ester−acid of the dianhydride was formed. After approximately 1 h, the excess ethanol was distilled from the solution, leaving a viscous yellow ester−acid mixture. An equimolar amount of the diamines (HMDA, 2.2326 g (19.21 mmol) and DoDDA, 3.8495 g (19.21 mmol)) was added to the ester−acid mixture along with NMP and *o*-DCB, an azeotroping solvent, to give 10 wt % solids. The solution was refluxed at 180 °C for 24 h to obtain fully cyclized imide linkages. The viscous solution was cooled and then added to stirring methanol. The white, fibrous material was isolated, washed with methanol, and dried under vacuum at 110 °C for 24 h.

Film Preparation. To fabricate films, the polyimides were dissolved in NMP to prepare 5−10% (w/v) solutions, filtered under pressure (argon, 60−80 psi) to remove impurities, and then degassed in a vacuum oven (air, 25 psi). The solutions were cast onto clean glass substrates using a doctor blade with a 25 mm clearance. The glass substrates were immediately placed onto a temperature programmable hot plate, covered, and exposed to a gentle flow of nitrogen. The temperature was gradually increased from 30 °C to (T_g + 10 °C) over 8 hours. Because the polyimides were fully imidized, the long heating cycle removed the NMP slowly enough to prevent the formation of bubbles within the films. Upon completion of the heating cycle, the films were removed from the glass substrates using a razor blade to lift an edge of the film, followed by applying several drops of water at the exposed interface to induce delamination. The resulting films were approximately 0.03 mm thick.

Characterization. Gel permeation chromatography (GPC) was conducted using a Waters GPC/ALC 150C chromatograph equipped with a differential refractometer detector and a differential viscometer detector (Viscotek 150R). Waters μStyragel HT3 + HT4 columns maintained at 60 °C were used. NMP, which contained 0.02 M P_2O_5, was the mobile phase (0.1 mL/min flow rate). A universal calibration curve was generated using a series of polystyrene standards with narrow molecular weight distributions such that absolute values of $\langle M_n \rangle$, $\langle M_w \rangle$, and $\langle M_v \rangle$ could be calculated.[20,21]

Degradation temperatures of the polyimides were found by heating 10-mg samples at 10 °C/min to 900 °C in air using a Perkin Elmer TGA 7 instrument.

A Perkin Elmer DSC 7 instrument was used to determine the glass transition temperature. Samples (10 mg) were heated at 10 °C/min to 300 °C under a nitrogen purge. Two heating cycles were performed, with the T_g reported obtained on the second scan.

Dynamic mechanical analysis (DMA) was utilized to determine the viscoelastic relaxation transition temperatures. A TA Instruments DMA 2980 was operated in the film tension geometry. Films, 20 × 5 × 0.03 mm, were tested at a frequency of 1 Hz and an oscillation amplitude of 20 μm. A heating rate of 2 °C/min over the temperature range of interest was utilized.

A TA Instruments DMA 2980 in the film tension geometry, creep mode, was utilized to measure the linear coefficient of thermal expansion (CTE). The dimension change of films, 20 × 5 × 0.03 mm, under 0.05 N of static force was monitored as a function of temperature. Multiple heating and cooling cycles, in which the temperature was ramped at 2 °C/min from 25 °C to just below the T_g, or vice versa, were performed. The T_g of the sample was not exceeded to prevent sample deformation during the temperature cycles. Liquid nitrogen was used to mediate the heating or cooling rate.

Dielectric analysis (DEA) experiments were performed using a TA Instruments DEA 2970. Films, 25.4 × 25.4 × 0.03 mm, were sputter coated with gold to improve their contact with the electrodes. A mask overlay was used to assist in sputtering a 285.05-mm^2 circle of gold on each side of the film, and the sputter time was set to coat 200 Å of gold. The ram force and minimum spacing were set to 150 N and 0 mm, respectively. A heating rate of 2 °C/min over the temperature range of interest was utilized, and seven decades of frequency, 0.1 to 100 000 Hz, were scanned. Two heating cycles were performed.

A Metricon Corporation model 2010 prism coupler was used to measure the in-plane refractive index. The instrument utilized a 200-P-4 prism and a He−Ne laser light source at a 632.8-nm wavelength. The index accuracy is ±0.001, and the index resolution is ±0.0005. Films, 20 × 5 × 0.03 mm, were tested at 25 °C, and five measurements were made for each sample.

Results and Discussion

The solubility of the fully cyclized polyimides allowed accurate molecular weight characterization of the entire series using GPC. Table 1 lists the molecular weights and polydispersities ($\langle M_w \rangle / \langle M_n \rangle$) for the different polyimide compositions. The data show that the ester−acid solution imidization produced high molecular weight polyimides, with the exception of BPADA/DCMH. The polydispersity values were around 2.2 for the series, which is typical for polycondensation reactions. Despite the low molecular weight of BPADA/DCHM, tough creasable films were easily prepared for property characterization. Wholly aromatic polyimides synthesized by the traditional two-step method are relatively insoluble; thus, the polyimide molecular weight has been typically estimated from the molecular weight data obtained for

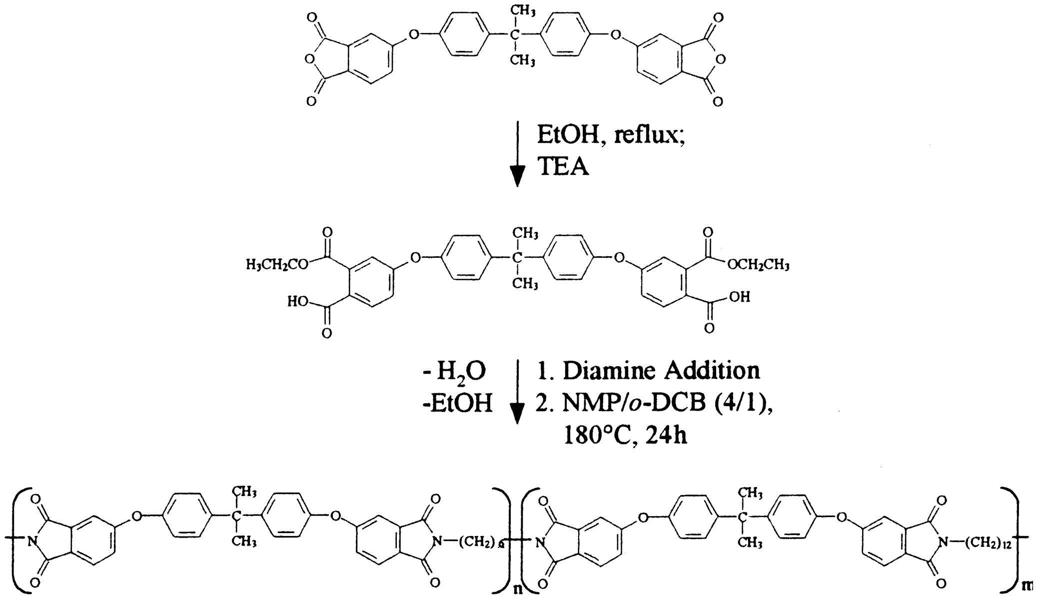

Figure 2. Ester–acid high-temperature solution imidization scheme.

Table 1. Molecular Weight and Thermal Characterization of BPADA-Based Polyimides

polyimide	diamine molar ratio	$\langle M_n \rangle$ kg/mol	$\langle M_w \rangle / \langle M_n \rangle$	T_g (°C) DSC[a]	T_{deg} (°C) TGA[b]
BPADA/ODA	1	54	2.9	224	514
BPADA/HMD–ODA (75:25)	0.75:0.25	81	2.3	150	458
BPADA/HMD–DoDDA (50:50)	0.50:0.50	27.3	1.9	103	465
BPADA/HMD–DoDDA (25:75)	0.25:0.75	36.7	2.2	88	452
BPADA/DCHM	1	6.6	1.9	205	450

[a] T_g reported from second heating cycle in nitrogen. [b] Five percent weight loss degradation temperature in air.

the soluble poly(amic acid) precursor.[2,4,6] In contrast, using GPC, molecular weight data for our fully cyclized soluble polyimides were relatively easy to determine and more accurate.

Table 1 also lists the glass transition temperatures and thermal degradation temperatures (5% weight loss in air) for the BPADA-based polyimides. The fully aromatic BPADA/ODA possessed the highest T_g and the best thermal stability, as expected. The high glass-transition temperature of BPADA/ODA is attributed to the rigid, predominantly aromatic, backbone structure and the formation of strong intermolecular complexes. The high thermal stability of BPADA/ODA is due to the high content of strong aromatic covalent bonds. Table 1 shows that as the aliphatic content increases the T_g and thermal stability decrease. The linear methylene groups of HMDA and DoDDA impart flexibility to the backbone and allow cooperative segmental motions associated with the T_g to initiate at lower temperatures. Whereas the thermal stability for these polyimides decreased because of the susceptibility of the methylene units to oxidative degradation, the lower T_g should facilitate melt processing.

The cycloaliphatic diamine, DCHM, is more rigid than HMDA and DoDDA; the increased main-chain rigidity is reflected in the high T_g of 205 °C, which is comparable to the T_g of the fully aromatic BPADA/ODA. Glass-transition temperatures of ~200 °C have been reported for similar aromatic dianhydride-based polyimides containing DCHM.[6,11] Table 1 also shows that the 5% weight loss temperature of BPADA/DCHM is 450 °C, which is comparable to the thermal stability of the other partially aliphatic polyimides. We note that the DCHM methylene units are incorporated within a ring structure such that a single C–C bond scission would not lead to an immediate significant decrease in molecular weight.[5,22] Conversely, for HMDA or DoDDA, methylene C–C bond scission would directly decrease the molecular weight. Thus, for limited extents of degradation, BPADA/DCHM mechanical properties may not be compromised at elevated temperatures.

The linear CTE is defined as the relative change in length divided by the change in temperarature

$$\alpha = \frac{1}{l_0}\left(\frac{\Delta l}{\Delta T}\right) \qquad (1)$$

where α is the linear CTE, l_0 is the initial sample length, Δl is the change in sample length, and ΔT is the change in temperature. From an atomistic perspective, the CTE reflects an increase in the average distance between atoms with increasing temperature.[23] The greater the atomic bonding energy, the less the interatomic distance will increase with temperature. Relative to aromatic covalent bonds, aliphatic covalent bonds have a lower average bond enthalpy and are thus expected to lengthen more with increasing temperature. Intermolecular interactions also act to resist dimension changes with increasing temperature, with high cohesive energy densities leading to a lower CTE.[24]

Figure 3 illustrates the change in sample dimension with temperature for BPADA/DCHM. The results shown in Figure 3 are representative of the BPADA-based polyimides. Three heating cycles and two cooling cycles are plotted. The first heating cycle is marked. The dimension change with temperature for the first heating cycle differs from the subsequent heating cycles and reflects the sample preparation history. During the first heating cycle, absorbed moisture and residual stresses were released. Figure 3 shows that the cooling curves

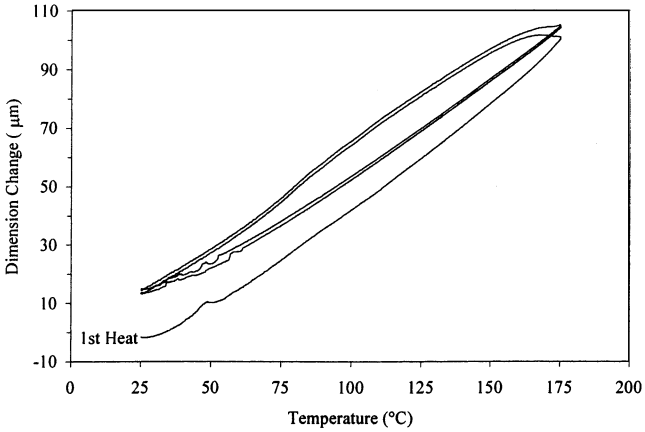

Figure 3. Dimension change vs temperature for BPADA/DCHM.

Table 2. Linear Coefficients of Thermal Expansion

polyimide	CTE (ppm/°C)
BPADA/ODA	31.0
BPADA/HMDA−ODA (75:25)	45.3
BPADA/HMDA−DoDDA (50:50)	51.5
BPADA/HMDA−ODA (25:75)	52.5
BPADA/DCHM	42.3

are different from the heating curves. This is due to thermal lag within the DMA furnace; if the heating/cooling rates are decreased, the envelope size will decrease. Using the initial sample length and slopes of the second and third heating cycles, the linear CTEs were calculated according to eq 1. The average linear CTE values are presented in Table 2.

Table 2 shows that as the aliphatic content increases, the CTE increases. The low CTE of BPADA/ODA is rationalized as due to the aromatic covalent bonds within its backbone and the intermolecular interactions between ODA and BPADA units on neighbor polyimide chains.[24,25] As the aliphatic content increases, the CTE increases because weaker covalent bonds within the polymer backbone are present and also weaker intermolecular interactions contribute. BPADA/DCHM possesses a CTE value slightly lower than that of BPADA/HMDA−ODA, 75:25. The cycloaliphatic DCHM units add rigidity to the main-chain that may facilitate the alignment of the segmental units, but they also participate in weaker, van der Waals intermolecular interactions. The aromatic ODA units add rigidity to the main-chain and add stronger intermolecular charge-transfer interactions with the BPADA units; however, because only 25% of the ODA is present in this copolyimide, its CTE is comparable to that of BPADA/DCHM. Table 2 shows that the CTE values for BPADA/HMDA−DoDDA, 50:50 and 25:75 are 51.5 and 52.5 ppm/°C, respectively. The CTE values are similar as expected from the similarity in chemical composition and structure. These CTE values are higher than for the other polyimides investigated because of the flexibility of the aliphatic units, which adds free volume, thus lowering intermolecular forces.

The viscoelastic relaxations of the BPADA-based polyimides were studied using DMA. A strong correlation was observed between the glass-transition temperature and the percent aliphatic content. These data were consistent with those determined from DSC. Figure 4 displays an overlay of log storage modulus (E') versus temperature for the five polyimides. Within Figure 4,

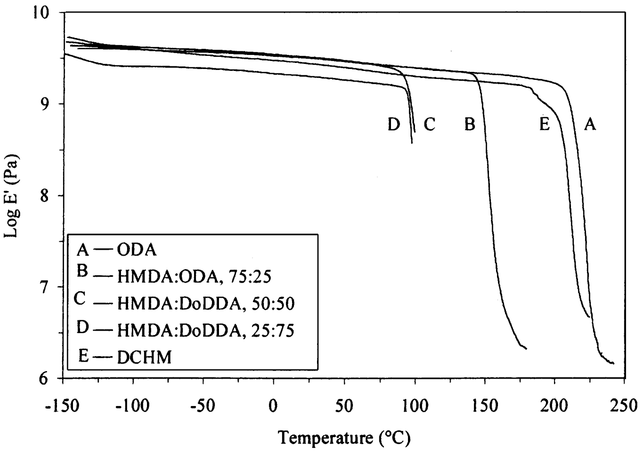

Figure 4. DMA, 1 Hz. The dependence of the storage modulus on the percent of aliphatic diamine.

Table 3. DMA Glass-Transition Temperatures, 1 Hz

polyimide	T_g (°C) storage modulus[a]	T_g (°C) tan delta[b]
BPADA/ODA	201	222
BPADA/HMDA−ODA (75:25)	143	156
BPADA/HMDA−DoDDA (50:50)	90	n/a
BPADA/HMDA−ODA (25:75)	91	n/a
BPADA/DCHM	199	215

[a] Onset temperature. [b] Peak maximum.

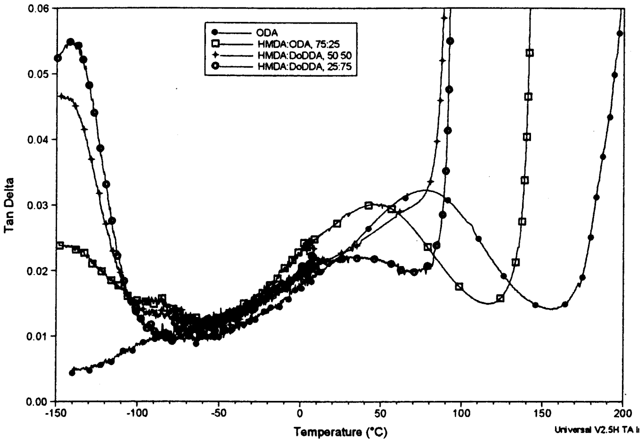

Figure 5. Sub-T_g DMA responses at 1 Hz for BPADA/ODA; BPADA/HMDA−ODA, 75:25; BPADA/HMDA−DoDDA, 50:50; and BPADA/HMDA−DoDDA, 25:75.

the E' curve for BPADA/DCHM shows a small decrease just prior to the glass transition. Recall that BPADA/DCHM possesses a low M_n of 6.6 kg/mol. Thus, at temperatures near the glass transition, film elongation is likely. The magnitude of E' for the polyimides is typical of glassy polymers, 10^9 Pa, and the E' for the polyimides containing ODA units are higher than for the predominately aliphatic polyimides. BPADA/HMDA−DoDDA, 50:50 showed an E' value comparable to that of the ODA-containing polymers, which was unexpected.

Table 3 lists the glass-transition temperatures calculated from the onset of the rapid decrease in the storage modulus (E') and also from the tan delta measurements. Sample elongation within the T_g for the 50:50 and 25:75 HMDA−DoDDA diamine samples prevented the acquisition of a complete tan delta peak.

DMA also revealed several sub-T_g, local viscoelastic relaxations (Figures 5 and 6). The variations in chemical composition are reflected in the tan delta signal. A

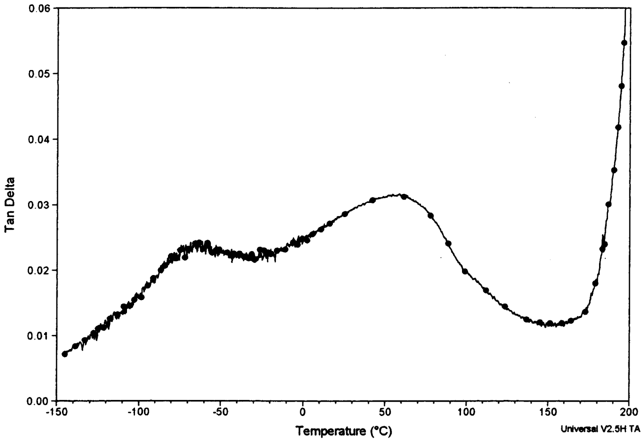

Figure 6. Sub-T_g DMA response at 1 Hz for BPADA/DCHM.

crankshaft motion (γ relaxation) attributed to the DoDDA and HMDA units is observed at ca. −140 °C (Figure 5). This assignment was made by comparison to prior viscoelastic studies of polyethylene.[26] The methylene unit cooperative crankshaft motions have also been observed within nylon-6,6, in polyesters, and in oxide polymers that contain linear $(CH_2)_{n\geq4}$ sequences that are separated by immobile groups.[26] Whereas the tan delta magnitude assigned to a crankshaft motion is composed of motions from both DoDDA and HMDA, the longer DoDDA sequences appear to be more influential. BPADA/ODA and BPADA/DCHM do not contain linear aliphatic diamines—no relaxation is observed at ca. −140 °C. The molecular source for the small relaxation at ca. −90 °C for BPADA/ODA and BPADA/HMDA−ODA, 75:25 has not been identified; however, the relaxation may arise from residual NMP within the film. This relaxation is not observed within the dielectric experiments in which two heating cycles were performed.

BPADA/ODA and BPADA/HMDA−ODA, 75:25 both exhibit sub-T_g viscoelastic relaxations (β relaxations), which heating initiates at ca. −47 °C, but display peak maxima at ~75 and 50 °C, respectively. A phenyl ring torsional rotation within the ODA units is assigned as the underlying molecular motion. This association was made by comparison to prior viscoelastic studies of partially aliphatic[10] and aromatic polyimides.[27−30] Also, we note that the peak maximum for BPADA/ODA is ~25 °C higher than for BPADA/HMDA−ODA, 75:25. This effect arises from the broadening of the distribution of relaxation times as the ODA content and the backbone rigidity increase. Similar observations are reported for the β relaxation of polycarbonate.[26] A relaxation within this temperature range is also observed within BPADA/HMDA−DoDDA, 25:75 but not within BPADA/HMDA−DoDDA, 50:50. This observation is peculiar because their chemical structures are so similar. Obviously the molecular source cannot arise from ODA units, so perhaps the flexibility arising from the higher DoDDA content allows ordering during film formation that is then detected in the DMA tan delta response.

Figure 6 shows that BPADA/DCHM exhibits sub-T_g viscoelastic relaxations at ca. −78 and 60 °C. The relaxation at −78 °C is suspected to arise from internal friction due to isomer changes within the cyclohexyl ring. Low-temperature mechanical and dielectric relaxations have been observed within polycyclohexyl alkylacrylate derivatives, and an axial−equatorial (chair−chair) isomer mechanism, or ring inversion, has been assigned as the molecular origin.[26,31] A major difference between these literature examples and our study is that the BPADA/DCHM cyclohexyl ring is within the polyimide backbone, rather than a side group. Thus, our assignment is preliminary. The location of the cyclohexyl maximum, however, has been shown to be remarkably insensitive to the molecular environment.[31] The molecular source of the BPDAD/DCHM relaxation at ~60 °C is not clear.

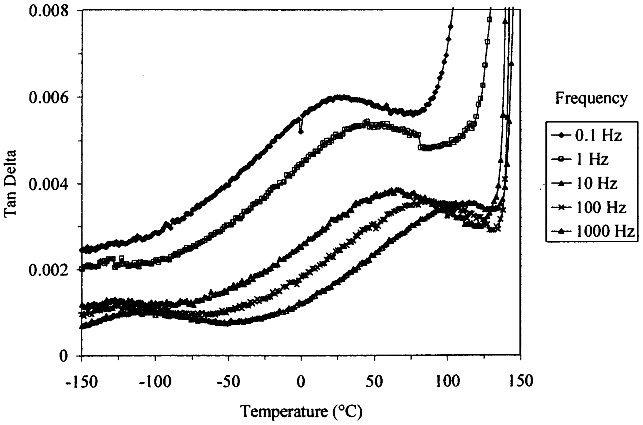

Figure 7. DEA, second heating. The frequency dependence of the γ and β relaxations for BPADA/HMDA−ODA, 75:25.

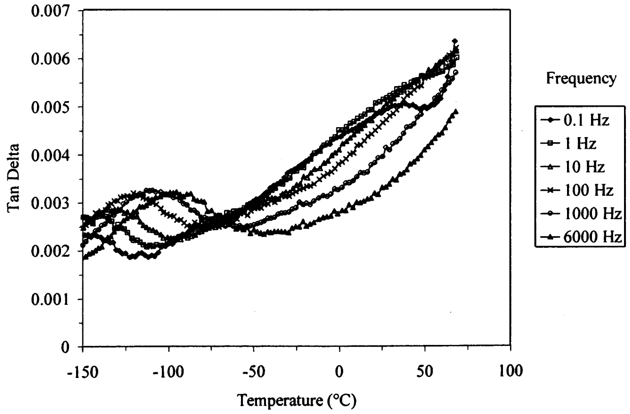

Figure 8. DEA, second heating. The frequency dependence of the γ relaxation for BPADA/HMDA−DoDDA, 25:75.

Examination of the viscoelastic properties by DEA also revealed two sub-T_g, local viscoelastic relaxations. A β relaxation for the polyimides containing ODA was observed at ~50 °C (1 Hz). A γ relaxation for the polyimides containing HMDA and DoDDA was observed at ca. −140 °C (1 Hz). Figures 7 and 8 present the dielectric tan delta signal frequency dependence of the sub-T_g relaxations for BPADA/HMDA−ODA, 75:25 and BPADA/HMDA−DoDDA, 25:75 respectively. For each polyimide, as the frequency increases, the relaxations shift to higher temperatures. Figure 9 shows the dielectric response of BPADA/DCHM; the shoulder at ca. −75 °C (0.1 Hz) is suspected to be due to isomer conformation changes within the cyclohexyl groups. At higher frequencies, the shoulder disappears because of overlap with the higher-temperature secondary relaxation.

The molecular origins of the sub-T_g relaxations identified from DMA are clarified by using data from the DEA sub-T_g relaxations in an Arrhenius activation energy analysis. The magnitude of an activation energy of a relaxation depends on rotation potential energy

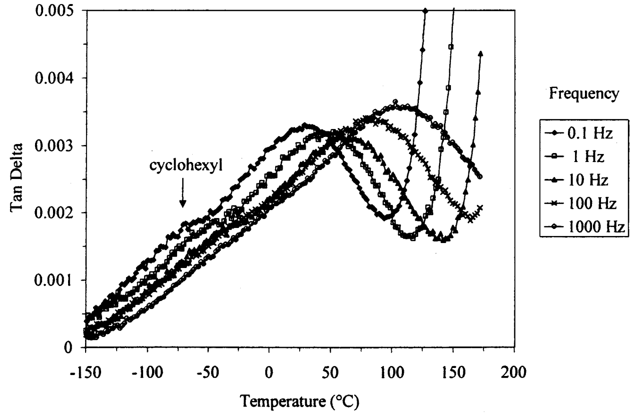

Figure 9. DEA, second heating. The frequency dependence of the sub-T_g relaxations for BPADA/DCHM.

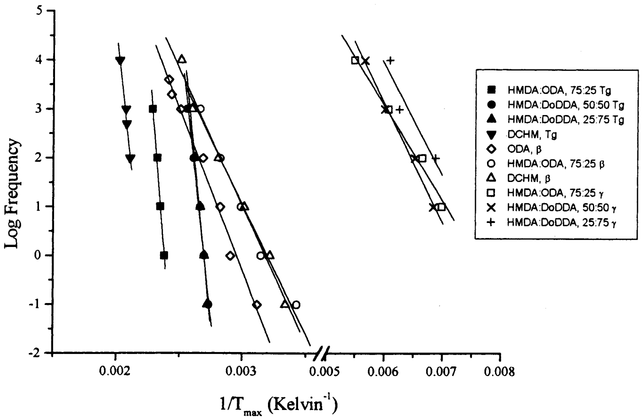

Figure 10. Log frequency vs 1/T for the DEA γ, β, and T_g relaxations of several BPADA-based polyimides. Note that the curves for the T_g of HMDA–DoDDA, 50:50 and HMDA–DoDDA, 25:75 overlay almost exactly.

barriers, internal friction, and the volume and environment of the moving repeat unit(s). An activation energy of a relaxation calculated from dielectric data is generally lower than the activation energy calculated for the same relaxation from mechanical data.[32] The activation energy for the glass transition, the β relaxation, and the γ relaxation for each of the polyimides was calculated by applying the Arrhenius equation

$$\omega = \omega_0 \exp(-E_a/RT) \tag{2}$$

where ω is frequency, ω_0 is the exponential prefactor, E_a is the activation energy, R is the gas constant, and T is the peak-maximum temperature. Figure 10 illustrates the log frequency versus 1/T relationships, and the best-fit lines distinguish the three types of relaxations. Within Figure 10, the slopes of the lines for the glass-transition temperatures are steeper than those for the β and γ relaxations. The high slope indicates a much higher activation energy and a different volume and environment of the moving segments. Table 4 presents the DEA Arrhenius activation energies calculated using the slopes of the best-fit lines.

The similarity in the activation energy for the γ relaxations suggests a common molecular origin. The γ relaxation E_a of ~43 kJ/mol (~10 kcal/mol) agrees reasonably well with the value of 11 kcal/mol reported for polyethylene and further confirms our assignment of a crankshaft motion.[26] The E_a values for the β relaxation are the same order of magnitude, and although the molecular origin for the BPADA/DCHM β relaxation differs from the ODA-containing polyimides, their relaxation volume-element size scales are similar. Mechanical and dielectric activation energies for the β relaxation of aromatic polyimides have been reported in the range 95–180 kJ/mol.[10,27,28] Table 4 also shows that the activation energies for the T_g are much higher than for the local, sub-T_g relaxations. This is characteristic of the thermal energy needed to activate the highly cooperative chain motions involved in the glass transition.[33]

Table 4. DEA Arrhenius Activation Energies

polyimide	activation energy (kJ/mol) gamma relaxation	 beta relaxation	T_g
BPADA/ODA	[a]	126.2	[c]
BPADA/HMDA–ODA (75:25)	44.0	101.4	591.8
BPADA/HMDA–DoDDA (50:50)	46.9	[a]	440.5
BPADA/HMDA–ODA (25:75)	37.1	[a]	499.4
BPADA/DCHM	[b]	106.7	443.6

[a] Relaxation not present. [b] Cyclohexane relaxation—a shoulder on the β. [c] Ionic conductivity obscured the T_g.

Table 5. Refractive Index and Dielectric Constant

polyimide	refractive index	dielectric constant via refractive index
BPADA/ODA	1.662	2.763
BPADA/HMDA–ODA (75:25)	1.633	2.667
BPADA/HMDA–ODA (50:50)	1.612	2.599
BPADA/HMDA–DoDDA (25:75)	1.607	2.582
BPADA/DCHM	1.598	2.554

Structure–property relationships for the refractive index and dielectric constant were also investigated. Polyimides with low dielectric constants are desirable to increase the efficiency at which a microelectronic device transmits signals. Polyimides containing more polarizable atoms or functional groups display a higher relative dielectric constant, ϵ_r, in all frequency ranges than polyimides with fewer polarizable groups. Table 5 lists the refractive indices and estimated relative dielectric constants (ϵ_r) for the BPADA-based polyimides. The ϵ_r values were estimated from the refractive indices using a relation deduced from Maxwell's equations:[34]

$$n^2 = \epsilon_r \tag{3}$$

where n is the refractive index and ϵ_r is the relative dielectric constant. This relation is applicable at optical frequencies (10^{15}–10^{16} Hz) where only electronic polarization occurs.

Table 5 shows that as the aromatic diamine content (ODA) decreases the refractive index also decreases; that is, the materials become more "transparent." The increased transparency is attributed to the reduction of charge-transfer complexes between neighbor polyimide chains and the reduction of extended conjugation along the polyimide backbone.[2,35] The polyimides with aliphatic and cycloaliphatic diamines possess comparable refractive index values. The low refractive index for BPADA/DCHM agrees well with literature examples. There, DCHM was suggested to prevent the occurrence of both inter- and intramolecular charge-transfer com-

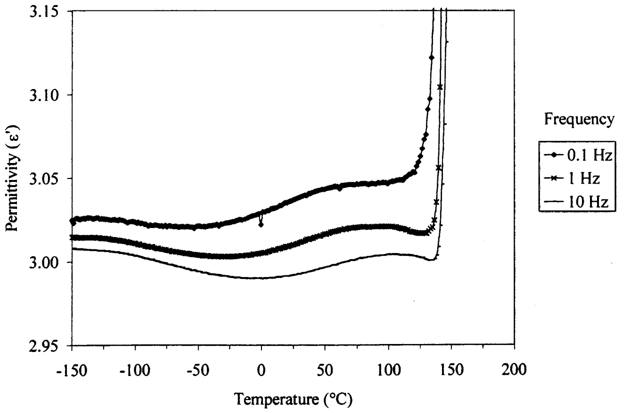

Figure 11. DEA, second heating. Permittivity response for BPADA/HMDA−ODA, 75:25.

plexes in polyimide films because of its weak electron-donating property.[5,7,11] Similar findings were reported for polyimides containing alkyl groups.[36] Table 5 also shows that the ϵ_r decreases with increasing aliphatic diamine content because of the presence of fewer polarizable functional groups. The decrease in chain linearity is also expected to contribute to the decrease in ϵ_r.[37,38]

The temperature dependence of the dielectric constant was examined from the DEA permittivity (ϵ') response. The permittivity response for BPADA/HDMA−ODA, 75:25 is illustrated in Figure 11. Figure 11 shows a step increase in the dielectric permittivity at the temperatures of the γ and β relaxations. The segmental mobility allows for alignment of the dipoles, which results in an increase in the permittivity and causes the material to become less insulative. The permittivity increase at the γ relaxation is ~0.015. The increase in the permittivity at the β relaxation is ~0.025. The difference in step-increase values reflects the difference in the molecular origin of the γ and β relaxations. The dipoles that align because of the crankshaft motion are very weak, and some dipolar contribution is thought to be from its near environment. Stronger dipoles are present within the ODA units, thus leading to a larger step increase. BPADA/ODA displayed a step increase of ~0.05 at the β relaxation, which reflects the greater number of ODA units. A step increase, ~0.015, at the temperature of the γ relaxation was similarly observed for the polyimides containing the diamines HMDA and DoDDA; for these polyimides, no correlation between the step increase value and the diamine content was noted. Figure 12 presents the temperature dependence of the permittivity response of BPADA/DCHM. The permittivity step increase is ~0.07; however, this increase contains contributions from the cyclohexyl and β relaxations.

The permittivity values displayed within Figures 11 and 12 are slightly higher than the room-temperature dielectric constants that were estimated from the refractive index (Table 5). The refractive index is measured at optical frequencies where only polarized electrons contribute to the dielectric constant; in contrast, the DEA values are measured at lower frequencies, where the polarization of dipoles and electrons contribute. In addition, the thin films (0.03 μm) analyzed showed a tendency towards static charging, which possibly also contributed to the DEA permittivity response.

Conclusions

High molecular weight, soluble, amorphous, partially aliphatic polyimide copolymers were synthesized via ester−acid high-temperature solution imidization. Chemical structure−physical property relationships were established. For the three polyimides—BPADA/ODA, BPADA/HMDA−ODA, 75:25, and BPADA/HMDA−DoDDA, 50:50—as the aliphatic content increased, the glass-transition temperature, thermal stability, refractive index, and dielectric constant decreased; however, the CTE increased. The physical properties of BPADA/HMDA−DoDDA, 50:50, and BPADA/ HMDA−DoDDA, 25:75 did not differ appreciably because of the similarity in chemical structure and aliphatic content. The molecular origins of the sub-T_g β and γ viscoelastic relaxations were investigated. A crankshaft motion within the HMDA and DoDDA unit was assigned to the γ relaxation, and a phenyl ring rotation within the ODA unit was assigned to the β relaxation.

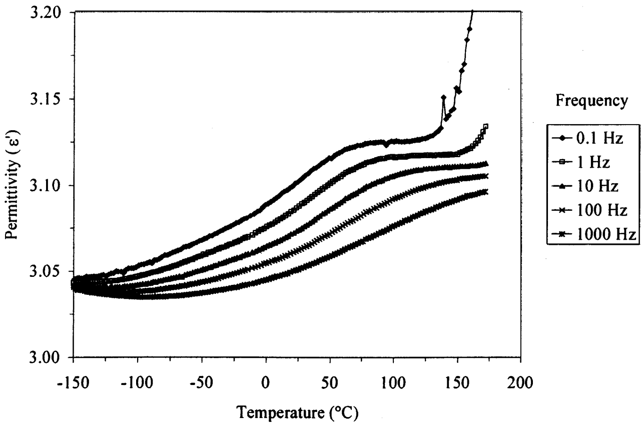

Figure 12. DEA, second heating. Permittivity response of BPADA/DCHM.

Relative to BPADA/ODA, BPADA/DCHM showed a decrease in thermal stability, refractive index, and dielectric constant and an increase in CTE; however, because of the rigidity of the DCHM, a comparable T_g value was observed. Two sub-T_g viscoelastic relaxations were detected. The relaxation at −78 °C is suggested to arise from isomer changes within the cyclohexyl ring. The molecular origin of the relaxation at 60 °C could not be assigned.

References and Notes

(1) Bessonov, M. I.; Koton, M. M.; Kudryavtsev, V.V.; Laius, L.A. *Polyimides Thermally Stable Polymers*; Consultants Bureau: New York, 1987; pp 245−259.
(2) *Polyimides*; Wilson, D., Stenzenberger, H.D., Hergenrother, P.M., Eds.; Blackie: London, 1990; pp 57−78.
(3) *Polyimides: Fundamentals and Applications*; Ghosh, M.K., Mittal, K.L., Eds.; Marcel Dekker: New York, 1996; pp 7−48, 71−120.
(4) Kreuz, J.A.; Hsiao, B.S.; Renner, C.A.; Goff, D.L. *Macromolecules* **1995**, *28*, 6926.
(5) Volksen, W.; Cha, H.J.; Sanchez, M.I.; Yoon, D.Y. *React. Funct. Polym.* **1996**, *30*, 61.
(6) Jin, Q.; Yamahita, T.; Horie, K.;Yokota, R.; Mita, I. *J. Polym. Sci., Polym. Chem. Ed.* **1993**, *31*, 2345.
(7) Jin, Q.; Yamahita, T.; Horie, K. *J. Polym. Sci., Polym. Chem. Ed.* **1994**, *32*, 503.
(8) Koning, C.; Delmotte, A.; Larno, P.; Van Mele, B. *Polymer* **1998**, *39*, 3697.
(9) Korshak, V. V.; Babchinitser, T. M.; Kazaryan, L. G.; Vasilyev, V. A.; Genin, Ya. V.; Azriel, A. Ye.; Vygodsky, Ya. S.; Churochkina, N. A.; Vinogradova, S. V.; Tsvankin, D. Ya. *J. Polym. Sci., Polym. Phys. Ed.* **1980**, *18*, 247.
(10) Eichstadt, A. E.; Ward, T. C.; Bagwell. M. D.; Farr, I. V.; Dunson, D. L.; McGrath, J. E. *J. Polym. Sci., Polym. Phys. Ed.* **2002**, *40*, 1503.
(11) Li, Q.; Horie, K.; Yokota, R. *Polym. J.* **1998**, *30*, 805.
(12) Chern, Y. T.; Shiue, H. C. *Macromolecules* **1997**, *30*, 5766.

(13) Moy, T. M. Ph.D. Dissertation, Virginia Tech, Blacksburg, VA, 1993.

(14) Moy, T. M.; DePorter, C. D.; McGrath, J. E. *Polymer* **1993**, *34*, 819.

(15) Tan, B. Ph.D. Dissertation, Virginia Tech, Blacksburg, VA, 1997.

(16) Tan, B.; Vasudevan, V.; Lee, Y. J.; Gardner, S.; Davis, R. M.; Bullions, T.; Loos, A. C.; Parvatareddy, H.; Dillard, D. A.; McGrath, J. E.; Cella, J. *J. Polym. Sci., Polym. Chem. Ed.* **1997**, *35*, 2943.

(17) Farr, I. V.; Glass, T. E.; Ji, Q.; McGrath, J. E. *High Perform. Polym.* **1997**, *9*, 345.

(18) Farr, I. V. Ph.D. Dissertation, Virginia Tech, Blacksburg, VA, 1999.

(19) Farr, I. V.; Kratzner, D.; Glass, T. E.; Dunson, D.; Ji, Q.; McGrath, J. E. *J. Polym. Sci., Polym. Chem. Ed.* **2000**, *38*, 2840.

(20) Konas, M.; Moy, T. M.; Rogers, M. E.; Schultz, A. R.; Ward, T. C.; McGrath, J. E. *J. Polym. Sci,. Polym. Phys. Ed.* **1995**, *33*, 1429.

(21) Konas, M.; Moy, T. M.; Rogers, M. E.; Schultz, A. R.; Ward, T. C.; McGrath, J. E. *J. Polym. Sci., Polym. Phys. Ed.* **1995**, *33*, 1441.

(22) Matsumoto, T. *Macromolecules* **1999**, *32*, 4933.

(23) Callister, W. D., Jr. *Materials Science and Engineering: An Introduction*, 3rd ed.; Wiley & Sons: New York, 1994; pp 646−648, 696−698.

(24) Liou, H. C.; Ho, P. S.; Stierman, R. *Thin Solid Films* **1999**, *339*, 68.

(25) Numata, S.; Kinjo, N. *Polym. Eng. Sci.* **1988**, *28*, 906.

(26) McCrum, N.G.; Read, B.E.; Williams, G. *Anelastic and Dielectric Effects in Polymeric Solids*; Dover: New York, 1991; pp 180−185, 353−389, 501−539.

(27) Arnold, F. E.; Bruno, K. R.; Shen, D.; Eashoo, M.; Lee, C. J.; Harris, F. W.; Cheng, S.Z.D. *Polym. Eng. Sci.* **1993**, *33*, 1372.

(28) Coburn, J. C.; Soper, P. D.; Auman, B. C. *Macromolecules* **1995**, *28*, 3253.

(29) Li, F.; Fang, S.; Ge, J. J.; Honigfort, P. S.; Chen, J. C; Harris, F. W.; Cheng, S. Z. D. *Polymer* **1999**, *40*, 4987.

(30) Li, F.; Fang, S.; Ge, J. J.; Honigfort, P. S.; Chen, J. C.; Harris, F. W.; Cheng, S. Z. D. *Polymer* **1999**, *40*, 4571.

(31) Heijboer, J. In *Molecular Basis of Transitions and Relaxations*; Meier, D.J., Ed.; Gordon and Breach Science: New York, 1978; pp 75−102, 297−310.

(32) Starkweather, H. W., Jr.; Avakian, P. *Macromolecules* **1989**, *22*, 4060.

(33) Starkweather, H. W., Jr. *Macromolecules* **1981**, *14*, 1277.

(34) Atkins, P. *Physical Chemistry*, 5th ed.; Freeman: New York, 1994; pp 761−762.

(35) Ando, S.; Matsuura, T.; Sasaki, S. *Polym. J.* **1997**, *29*, 69.

(36) St. Clair, A. K.; Slemp, W. S. *SAMPE J.* **1985**, *21*, 28.

(37) Eftekhari, A.; St. Clair, A. K.; Stoakley, D. M.; Sprinkle, D. R.; Singh, J. J. In *Polymers for Microelectronics: Resists and Dielectrics*; Thompson, L.F., Wilson, C. G., Tagawa S., Eds.; ACS Symposium Series 537; American Chemical Society: Washington, DC, 1994; pp 535−545.

(38) Simpson, J. O.; St. Clair, A. K. *Thin Solid Films* **1997**, *308−309*, 480.

MA020835P